Available online at www.sciencedirect.com
SCIENCE DIRECT
Journal of Pharmaceutical and Biomedical Analysis 39 (2005) 404–410
JOURNAL OF PHARMACEUTICAL AND BIOMEDICAL ANALYSIS
www.elsevier.com/locate/jpba

Interaction of daunomycin antibiotic with human serum albumin: Investigation by resonant mirror biosensor technique, fluorescence spectroscopy and molecular modeling methods

Kai Tang, Yi-Min Qin, Ai-Hua Lin, Xing Hu, Guo-Lin Zou *

Key Laboratory of MOE for Virology, College of Life Sciences, Wuhan University, Wuhan 430072, China

Received 20 December 2004; received in revised form 13 March 2005; accepted 17 March 2005
Available online 17 June 2005

Abstract

Daunomycin (DM) is a clinically used antitumor anthracycline antibiotic, which is transported primarily by human serum albumin (HSA) in the blood. Binding characteristics are therefore of interest for both the pharmacokinetics and pharmacodynamics of DM. A new optical biosensor technique based on the resonant mirror was used to characterize interaction of DM with HSA at different temperatures and the affinity constants were obtained. The HSA–DM interaction is exothermic with having favorable enthalpy and entropy followed by the integrated van't Hoff equation analysis. Fluorescence studies showed that DM has an ability to quench the intrinsic fluorescence of HSA through a static quenching procedure according to the Stern–Volmer equation and DM displays a pH-dependent binding affinity to HSA. Molecular modeling calculations showed that the DM binds HSA to a non-classical drug binding site and further analysis of the binding site of DM within the HSA molecule suggested that hydrophobic contacts, hydrogen bond formation and electrostatic interactions account for the binding of DM.

Keywords: Human serum albumin; Daunomycin; Resonant mirror biosensor; IAsys; Binding thermodynamics; Fluorescence quenching

1. Introduction

Human serum albumin (HSA) is a principal carrier protein in serum known to bind a wide variety of endogenous and exogenous compounds with dissociation binding constants (K_D) in the range of 10^{-3} to 10^{-8} mol l^{-1} [1]. The binding form of the drug and the serum albumin is the storage form for the drug. It is important to study the interaction of the drug with the protein because protein–drug binding plays an important role in pharmacology and pharmacodynamics. The structural features of HSA are now well documented. It is well known that HSA is a helical monomer of 66 kDa containing three homologous domains (I–III) each of which is composed of A and B subdomains [2]. The two major drug binding sites of HSA named sites I and II are located in hydrophobic cavities in subdomains IIA and IIIA [2,3].

Anthracycline antibiotics are widely used in chemotherapy [4]. The reversible binding of anthracyclines to serum components was previously observed, and serum albumin was suggested to be the major ligand for this family of drug [5–7]. The parent compounds of this group are adriamycin (ADR) and daunomycin (DM). The interaction of ADR with HSA has been characterized in detail [5]. However, progress in understanding anthracycline antibiotics binding has been hampered, due largely to the instability of anthracycline antibiotics. Experimental evidence indicated that ADR frequently undergoes considerable degradation in aqueous solution (~40% in 24 h at 310 K) [5]. Early work on the binding of anthracyclines to serum albumin, which concentrated on characterizing the capacity and affinity of the protein for anthracyclines, identified different affinities by using equilibrium dialysis and ultrafiltration ($K_D \approx 10^{-4}$ to 10^{-5} mol l^{-1})

* Corresponding author. Tel.: +86 27 87645674; fax: +86 27 87669560.
E-mail address: zouguolin@whu.edu.cn (G.-L. Zou).

0731-7085/$ – see front matter © 2005 Elsevier B.V. All rights reserved.
doi:10.1016/j.jpba.2005.03.045

[6,7]. Although these traditional methods are straightforward, they are usually time-consuming and require many controls. Additionally, these techniques are based on analysis of free drug. As a consequence, the relative degradation of anthracycline antibiotic can have significant influence on binding analysis.

Drug binding to HSA has been studied by numerous methods. Current high-performance affinity chromatography, capillary electrophoresis and surface plasmon resonance are widely applicable for such work. Compared to conventional methods such as equilibrium dialysis and ultrafiltration methods, the use of these techniques may offer several advantages. Important advantages are small sample size and relatively short analysis time [8–10]. More recently, IAsys biosensor, which is based on the resonant mirror principle, has also been recognized as a powerful tool in monitoring the interaction between a small molecule and HSA with advantages of no labeling, real-time and non-invasive measurements [11–13]. In this approach, real-time binding of small molecules to immobilized HSA covalently attached to the carboxylate cuvette is monitored as a change in refractive index occurring at the surface of the biological layer and is directly proportional to the amount of bound small molecules. This advanced technology is used in rapidly and accurately determining binding parameters. The commercially available IAsys Autoplus biosensor system offers rapid temperature equilibration allowing the real-time study of the effect of temperature in binding studies. So IAsys biosensor can give complementary thermodynamic information to microcalorimetry, since only the direct binding is measured with IAsys whereas microcalorimetry measures all components in biomolecular interactions, including, e.g. hydration effects.

DM (Fig. 1) is an amphiphilic molecule possessing the dihydroxyanthraquinone ring system and the amino sugar moiety bound at C(7) site, which bears the positive electrostatic charge localized at protonated amino nitrogen. The amino sugar moiety with pK_a of 8.4 at 298 K is critical for the concentration of the neutral form of the drug. Despite the similarities in molecular structure of the ADR and DM, the latter is more lipophilic [14]. There is to date no report concerning the protein–DM binding assay by using IAsys biosensor. In the present paper, the extended studies on the interaction of DM with HSA were performed. The IAsys biosensor and fluorescence spectroscopy were combined to investigate the HSA–DM complex with the goal of obtaining information about the effects of temperature and pH on affinity constants. The DM binding mode to HSA was studied using automated molecular docking approach. Experimental observations and theoretical data could be helpful to understand transports of DM in the blood.

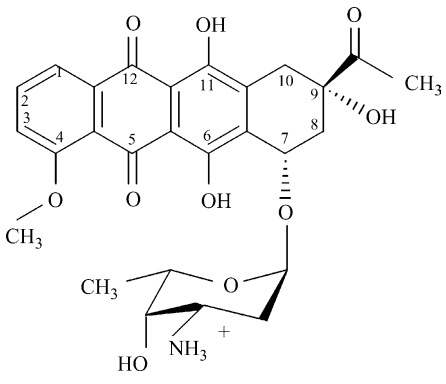

Fig. 1. The chemical structure of daunomycin (DM).

2. Materials and methods

2.1. Materials

Human serum albumin (fatty acid free <0.005%) and daunomycin, purchased from Sigma Chemical Company, were used without further purification. The planar IAsys carboxylate cuvette was from Affinity Sensors (Cambridge, UK). Ethanolamine, *N*-hydroxysuccinimide (NHS) and *N*-ethyl-*N*′-(3-dimethylaminopropyl)carbodiimide hydrochloride (EDC) were supplied as NHS coupling kit by Affinity Sensors. Phosphate-buffered saline (PBS), final pH 7.4, was prepared for IAsys measurements and 0.01 mol l^{-1} sodium acetate buffer (pH 5.0) for immobilization of HSA on the surface of carboxylate cuvette. The 0.05 mol l^{-1} Tris–HCl (pH 7.4 and 8.4), and 0.01 mol l^{-1} sodium acetate buffer (pH 5.4) had been used for the fluorescence titration experiments and the ionic strengths of buffers were adjusted to 0.15 mol l^{-1} with sodium chloride. HSA stock solutions were prepared in different buffers and kept at 4 °C. The concentrations of the protein were determined by measuring the UV absorbance of the solutions at 280 nm, using an extinction molar coefficient of 36,600 l mol^{-1} cm^{-1} [15]. Stock solution of DM was prepared in water and stored at −20 °C in the dark. The concentration of DM was calculated by using a molar absorption coefficient at 480 nm equal to 11,500 l mol^{-1} cm^{-1} [16]. Analytical grade reagents were used to prepare the buffers, and water treated with Milli-Q system (Millipore, USA) was used for all the experiments. The pH was measured with HI98103 digital pH-meter (Hanna, Italy) and a Cary 5000 spectrophotometer (Varian, USA) was used in UV–vis absorption measurements.

2.2. IAsys optical biosensor measurements

IAsys affinity sensor analysis experiments were conducted on the IAsys Autoplus (Affinity Sensors, Cambridge, UK), a fully automated optical evanescence resonant mirror cuvette system. The data were collected at the fastest data collection rate (0.3 s^{-1}) and the stirring rate was set to 100 rpm in order to minimize mass transport effects. HSA were covalently coupled to sensor chips via free amino groups using EDC/NHS at 295 K according to the manufacturer's instructions [17]. All binding reactions were carried out in phosphate-buffered saline at six temperatures (285, 288, 293, 298, 303, 310 K).

After equilibrating the cuvette with binding buffer, varying concentrations of DM were added, and each binding response was monitored during the "association" phase. Following each cycle of analysis, the cuvette was regenerated by washing with 1.0×10^{-5} mol l^{-1} NaOH [18], and baseline was reestablished with binding buffer. IAsys FASTfit software, Version 2.03 (Affinity Sensors, Cambridge, UK) was used to fit the experimental data according to the procedures described in the software manual, which provided the values of observed binding rate (k_{on}) at each DM concentration.

2.3. Fluorescence measurements

Fluorescence spectroscopy measurements were performed using a LS-55 luminescence spectrometer (Perkin-Elmer, CT) equipped with a thermostatically controlled cell holder. The excitation wavelength of 280 nm was used, and the emission spectra were obtained from 300 to 390 nm. Both excitation and emission slit widths were 5 nm, and the scan speed was 120 nm min^{-1}.

Fluorescence experiments were carried out at 298 K. A 3.0-ml sample of 1.0×10^{-6} mol l^{-1} HSA solution at different pH values of 5.4, 7.4 and 8.4 was placed in a 1 cm quartz fluorescence cuvette and titrated with 3-μl aliquots of 2.0×10^{-4} mol l^{-1} DM with continuous stirring. The samples were equilibrated until a steady emission reading was obtained. The accumulated volume of titration was less than 50 μl, so the dilution effect was negligible.

2.4. Molecular modeling calculations

The program AutoDock 3.05 was used in this docking study, which uses a force field-based empirical free energy scoring function [19]. All molecular modeling and docking simulations were performed on a 16 CPU SGI workstation. The crystal structure of HSA entitled 1H9Z was taken from the Brookhaven Protein Data Bank (http://www.rcsb.org/pdb) [20]. The 3D structure of DM was obtained from the NCI DIS 3D database (http://dtp.nci.nih.gov).

The geometry of DM was optimized using the Tripos force field with Gasteiger–Hückel charges by software Sybyl 6.9.2 [21]. The structure of HSA was assigned according to the Amber 4.0 force field with Kollman-united-atom charges encoded in Sybyl 6.9.2. The solvation parameters were added to protein using Addsol modules of AutoDock. Grid maps were generated with 0.375 Å spacing by the Autogrid program for the whole protein target. The Lamarckian genetic algorithm (LGA) was applied to deal with the HSA–DM interaction. Random starting positions, orientations and torsions (for flexible bonds) were used for the ligand, each docking run consisted of 100 cycles. The docked complexes were selected according to the criteria of interacting energy combined with geometrical matching quality. The MOLCAD implemented in Sybyl 6.9.2 software package was used to visualize the environment of binding pocket.

3. Results and discussions

3.1. Binding constants derived from the IAsys biosensor

To carry out the biosensor assays, human serum albumin was first attached to the sensor chip and its interaction with the daunomycin was tested. HSA was coupled to the cuvette giving a signal of 530 arcsec, corresponding to 12.4 ng of protein according to the guidelines supplied by the manufacturer (Fig. 2).

IAsys technology was used to measure the rate constants at temperatures ranging from 285 to 310 K. The temperature range chosen was such that HSA does not undergo any structural degradation in this range [22] and the binding activity of immobilized HSA is not influenced. In Fig. 3A, association curves recorded for 10 concentrations of DM at 293 K are shown and the obtained data were used to calculate an association rate (k_a) and a dissociation rate (k_d) (Fig. 3B). The dissociation equilibrium constant (K_D) was then derived for each reaction from the equation:

$$K_D = \frac{k_d}{k_a} \quad (1)$$

A dissociation equilibrium constant for the HSA–DM interaction was estimated to be $K_D = (8.68 \pm 0.72) \times 10^{-6}$ mo1 l^{-1} at the temperature of 293 K, suggesting the binding of DM to albumin occurred with relatively high affinity. Our recent studies have also clearly demonstrated the formation of serum albumin–adriamycin (ADR) complex with lower affinity $K_D = (1.20 \pm 0.13) \times 10^{-5}$ mo1 l^{-1} by using IAsys [23]. Although DM bears exactly the same charge as ADR, however, the dihydroxyanthraquinone moiety is more liphophilic, therefore, the relative strong hydrophobic interaction contributes to the enhanced affinity relative to ADR. The HSA–DM complex is more stable at lower temperatures, as shown by the lower K_D (see Table 1).

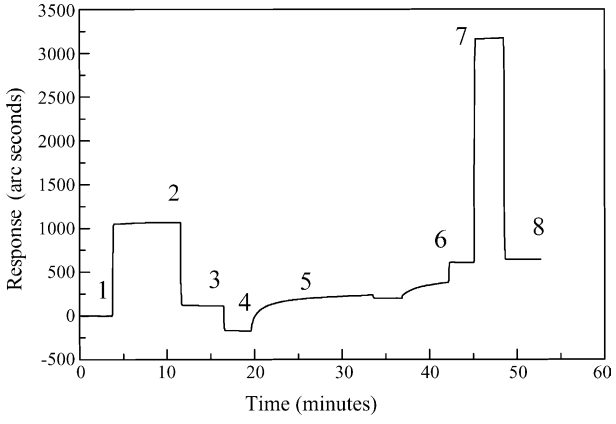

Fig. 2. Immobilization of human serum albumin (HSA) on the surface of carboxylate cuvette: (1) buffer baseline stabilization; (2) EDC/NHS mixture add; (3) buffer washes to remove unreacted molecules; (4) acetate buffer re-equilibration; (5) HSA in acetate buffer add; (6) buffer washes to allow dissociation; (7) block of non-coupled activated sites with ethanolamine; (8) baseline stabilization.

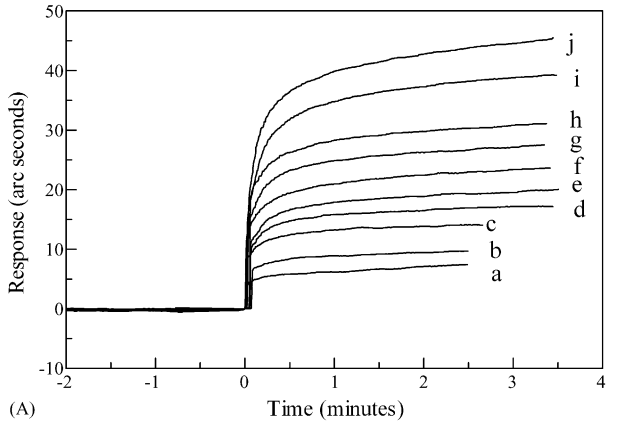

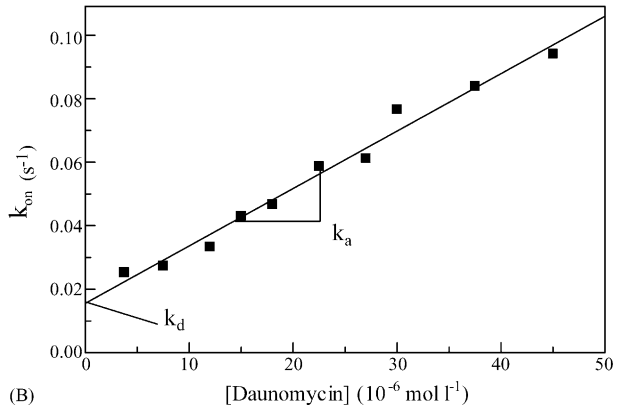

Fig. 3. Affinity measurements of DM for immobilized HSA at 293 K. (A) Association of DM to immobilized HSA led to the increase of the response as a function of time. The association phase were recorded for DM concentrations (a–j): 3.75×10^{-6}, 7.5×10^{-6}, 1.2×10^{-5}, 1.5×10^{-5}, 1.8×10^{-5}, 2.25×10^{-5}, 2.7×10^{-5}, 3.0×10^{-5}, 3.75×10^{-5} and 4.50×10^{-5} mol l^{-1}. (B) Calculation of the obtained data from the curves allowed the determination of the dissociation rate constant k_d from the ordinate intercept and the association rate constant k_a from the slope of the graph.

3.2. Thermodynamic analysis

From the temperature dependence of the equilibrium dissociation constants, it is possible to calculate values for the thermodynamic functions involved in the binding process. The change in free energy (ΔG) is related to the enthalpy (ΔH), entropy (ΔS) and normalized equilibrium association constant (K_A: $K_A = 1/K_D$) in the standard state (1 mol l^{-1}) according to:

$$\Delta G = \Delta H - T\,\Delta S = -RT\,\ln K_A \quad (2)$$

where R is the universal gas constant (8.314 J mol^{-1} K^{-1}) and T is the absolute temperature in Kelvin. ΔH and ΔS values corresponding to the binding of biological macromolecules very often show a significant temperature variation, resulting in a non-zero value of the heat capacity change (ΔC_p). ΔC_p may significantly differ from zero even if the linear correlation coefficient between $\ln K$ and $1/T$ is as high as 0.98 [24,25]. Within the limited range of temperatures relevant for the study of such associations, ΔC_p itself does not vary with temperature:

$$\Delta H(T) = \Delta H_0 + \Delta C_p(T - T_0) \quad (3)$$

where T_0 is some arbitrary chosen reference temperature (usually in the midrange of the interval). In order to include the temperature variation of enthalpy, the integrated form of van't Hoff equation should be used [25]:

$$\ln K = \ln K_0 + \left(\frac{\Delta H_0 - T_0\,\Delta C_p}{R}\right)\left(\frac{1}{T_0} - \frac{1}{T}\right) + \frac{\Delta C_p}{R}\,\ln\left(\frac{T}{T_0}\right) \quad (4)$$

Since in the temperature intervals accessible in our experiments never differed more than 7% from the average temperature (T_0), it was possible to expand the second term of Eq. (4) in a Taylor series of powers of $\theta = T/T_0 - 1$ [26]:

$$\ln K = A + B\theta + C\theta^2 \quad (5)$$

where $A = \ln K_0$, $B = \Delta H_0/RT_0$ and $C = -\Delta H_0/RT_0$ or $\ln K_0 = A$, $\Delta H_0 = BRT_0$ and $\Delta C_p = 2R(B + C)$. A multiple linear regression fit of the experimental data yields A, B and C at the reference temperature 298 K, and then ΔH_0, ΔC_p are obtained. Thus, the values of ΔH at different temperature are also could be achieved according to Eq. (3). The binding free energy, coupled with the binding enthalpy derived from the fitted van't Hoff data can calculate the corresponding entropic contributions to binding (ΔS). The thermodynamic binding profiles are also summarized in Table 1.

Only a small change in ΔG resulting from enthalpy-entropy compensation is observed over the temperature range studied. The thermodynamics of DM binding to HSA associated with favorable changes in both enthalpy and entropy show that binding is exothermic.

Table 1
Affinity constants for the interaction of DM with HSA obtained in IAsys experiments and corresponding thermodynamic parameters

Temperature (K)	K_D (mol l^{-1})	ΔG (kJ mol^{-1})	ΔH (kJ mol^{-1})	ΔS (J mol^{-1} K^{-1})
285	$(7.46 \pm 0.65) \times 10^{-6}$	-27.97 ± 0.21	-9.60 ± 2.43	64.46 ± 8.56
288	$(8.13 \pm 0.57) \times 10^{-6}$	-28.06 ± 0.17	-11.39 ± 1.91	57.90 ± 6.66
293	$(8.68 \pm 0.72) \times 10^{-6}$	-28.39 ± 0.20	-14.36 ± 1.11	47.88 ± 3.85
298	$(9.60 \pm 0.34) \times 10^{-6}$	-28.63 ± 0.09	-17.34 ± 0.65	37.90 ± 2.20
303	$(1.11 \pm 0.06) \times 10^{-5}$	-28.75 ± 0.14	-20.31 ± 1.11	27.85 ± 3.69
310	$(1.35 \pm 0.10) \times 10^{-5}$	-28.89 ± 0.19	-24.48 ± 2.26	14.24 ± 7.32

The heat capacity change upon binding was estimated to be $-0.60 \pm 0.18\,\mathrm{kJ\,mol^{-1}\,K^{-1}}$, indicating that there is a hydrophobic desolvation effect upon binding [27]. The classical view is generally accepted that positive entropy is taken as evidence for hydrophobic interaction from the structuring of the water molecule [28]. So the hydrophobic effect is clearly involved in DM binding to HSA. However, specific electrostatic interactions between ionic species in aqueous solution are characterized by a positive value of ΔS and a negative value of ΔH. Accordingly, it is not possible to account for the thermodynamic parameters HSA–DM complex on the basis of a single intermolecular force model. It is more likely that the presence of hydrogen bonding and electrostatic interactions contribute to binding [29].

3.3. Fluorescence quenching

A single tryptophan residue, Trp214, located in the depth of subdomain IIA of HSA is largely responsible for the intrinsic fluorescence of HSA. Fig. 4A shows fluorescence emission spectra for HSA in the presence of increasing of DM. No change of the fluorescence intensity was observed for the control HSA solution in these experiments. DM causes a decrease in the protein tryptophan fluorescence quantum yield. The possible quenching mechanism can be interpreted by the fluorescence quenching spectra of HSA and the F_0/F–[Q] (Stern–Volmer) curves of HSA with DM at different pH values as shown in Fig. 4B, where F_0 and F are the fluorescence intensities in the absence and presence of DM, respectively [Q], is the concentration of DM.

The Stern–Volmer plots are linear, indicating that only one type of quenching process occurs, either static or dynamic quenching [30]. In order to distinguish them, the procedure was assumed to be dynamic quenching. The quenching equation is presented by [30]:

$$\frac{F_0}{F} = 1 + K_q \tau_0 [Q] = 1 + K_{sv}[Q] \tag{6}$$

where K_{sv} is the Stern–Volmer constant, which is a direct measure of the quenching efficiency, K_q the quenching rate constant of the biomolecule, τ_0 is the average lifetime of the biomolecule. K_{sv} is obviously given by:

$$K_{sv} = K_q \tau_0 \tag{7}$$

where the fluorescence lifetime of the biopolymer τ_0 is 10^{-8} s [31], K_{sv} is the slope of linear regressions of Fig. 4B. According to Eq. (7), the quenching constant K_q can be obtained and are listed in Table 2 together with the correlation coefficients. However, the maximum scatter collision quenching constant K_q of various quenchers with the biopolymer is $2.0 \times 10^{10}\,\mathrm{l\,mol^{-1}\,s^{-1}}$ [32]. Obviously, the rate constant of protein quenching procedure initiated by DM is greater than the K_q of the scatter procedure. This means that the quenching is not initiated by dynamic collision but from the formation of a complex. For static quenching, the following

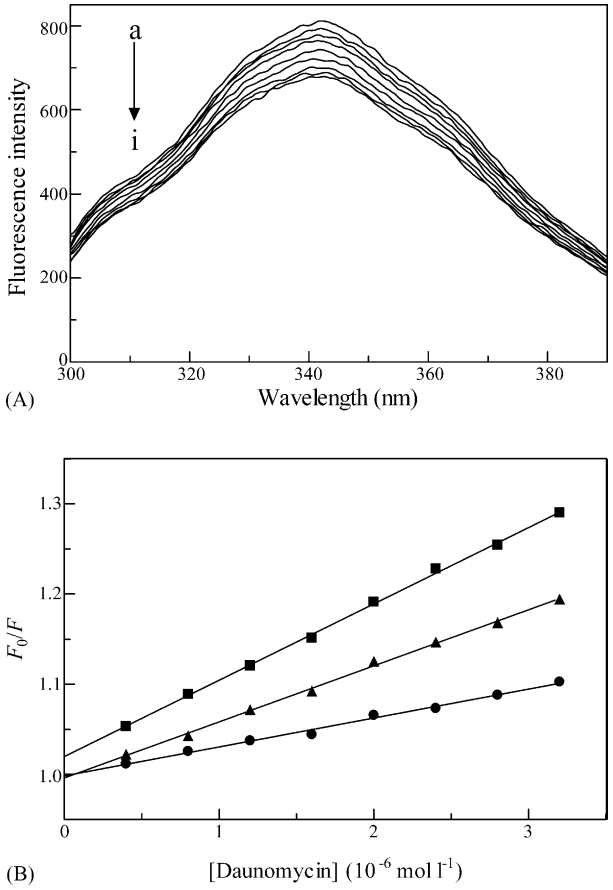

Fig. 4. Fluorescence quenching measurements of the binding of DM to HSA. (A) Fluorescence spectra for HSA at pH 7.4. The concentration of HSA is $1.0 \times 10^{-6}\,\mathrm{mol\,l^{-1}}$. Excitation was at 280 nm with the emission maximum at 341 nm. DM causes a concentration-dependent quenching of the intrinsic protein tryptophan fluorescence. The concentrations of DM were (a–i): 0, 0.4×10^{-6}, 0.8×10^{-6}, 1.2×10^{-6}, 1.6×10^{-6}, 2.0×10^{-6}, 2.4×10^{-6}, 2.8×10^{-6} and $3.2 \times 10^{-6}\,\mathrm{mol\,l^{-1}}$. (B) Stern–Volmer plots of the quenching of fluorescence of HSA by DM at different pH. The pH values were 5.0 (solid circle), 7.4 (solid triangle) and 8.4 (solid square), respectively. Data for each titration were analyzed by least-squares regression using GraphPad Prism 4.01 (GraphPad, CA).

equation was employed to calculate the dissociation binding constant [33]:

$$\frac{1}{F_0 - F} = \frac{1}{F_0} + \frac{K_D}{F_0\,[Q]} \tag{8}$$

The binding data (K_D) at different pH presented in Table 2 show that the binding of DM to HSA is found to increase with increasing pH. It was suggested that ligand in the

Table 2
The values of dynamic quenching constants and dissociation binding constants at all pH values examined

pH	K_q (l mol^{-1} s^{-1})	R	K_D (mo1 l^{-1})	R
5.4	$(3.13 \pm 0.14) \times 10^{12}$	0.9930	$(2.33 \pm 0.16) \times 10^{-5}$	0.9962
7.4	$(6.23 \pm 0.12) \times 10^{12}$	0.9979	$(1.41 \pm 0.11) \times 10^{-5}$	0.9934
8.4	$(8.47 \pm 0.12) \times 10^{12}$	0.9989	$(3.76 \pm 0.28) \times 10^{-6}$	0.9955

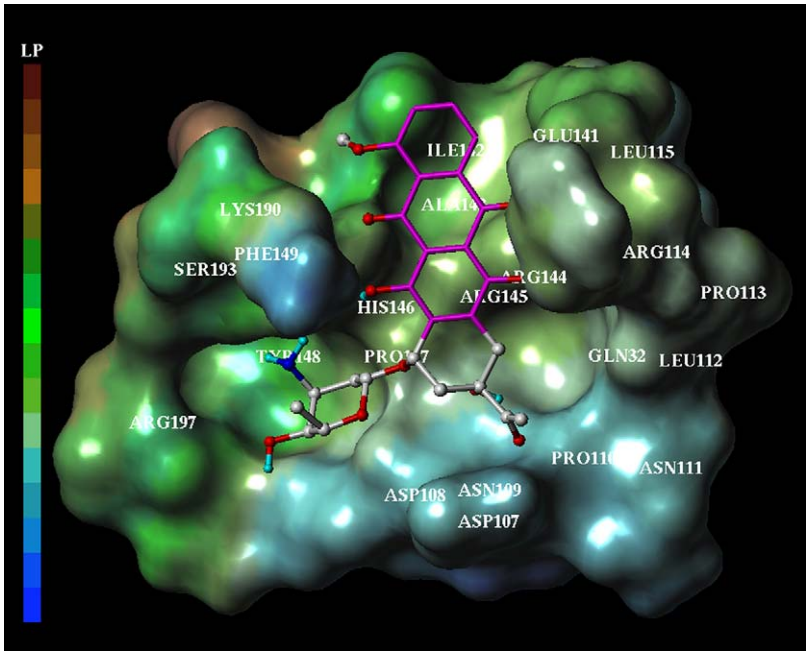

Fig. 5. Computer generated model of DM bound to HSA. The DM is represented by ball-and-stick (carbon, grey; nitrogen, blue; oxygen, red) and the anthraquione rings are colored by purple. The binding pockets residues of protein are represented by the lipophilicity of MOLCAD surfaces. The meanings of these color ramps are explained as the follows: it is the highest lipophilic area of the molecule in brown, while it is the highest hydrophilic area in blue. (For interpretation of the references to color in this figure legend, the reader is referred to the web version of this article.)

deprotonated form (pH 8.4) has a markedly higher affinity for HSA than the protonated form (pH 5.4), indicating that there is a contribution to the binding arising from electrostatic or hydrogen bonding interaction. Binding of carbamazepine (pK_a, 9.2) to HSA was characterized by high-performance affinity chromatography [34]. Interestingly, the interaction of carbamazepine with HSA was not sensitive to variations in pH, implying that electrostatic interaction did not play a major role in the binding of carbamazepine to HSA. It should be noted that the value of $K_D = (1.41 \pm 0.11) \times 10^{-5}$ mol l^{-1} under physiological pH conditions is higher than that obtained previously by kinetic analysis method, however, this fact can be attributed to substantial differences in experimental methods [35].

The fluorescence studies have shown that DM binds to HSA weaker than riboflavin binding protein (RBP) [36]. The X-ray crystallographic studies on RBP suggested that the larger and deeper cavity could be the high affinity site ($K_D = 5 \times 10^{-7}$ mol l^{-1}) for DM [37]. The great fluorescent spectrum of DM change is due to the embedding of the dihydroxyanthraquinone moiety inside the hydrophobic cavity [38]. On the other hand, the small changes found in DM spectra upon binding HSA (data not shown) point to a preferential location on the "surface" site.

3.4. Computational modeling of the HSA–DM complex

Although solution experiments may more closely represent physiological conditions, it is difficult to determine the location of the binding sites. The Autodock program was chosen to examine the binding mode of DM at the active site of HSA. The best docking energy result is shown in Fig. 5. As can be seen, DM is situated at the surface binding site in subdomain IB where Ile142, Ala143, Pro147 can make hydrophobic with phenol ring of DM. The interaction between DM and HSA is not exclusively hydrophobic in nature since there are several ionic (His146, Arg144, Arg145, Lys190, Arg197) and polar residues (Asn109, Leu115, Ser193) in the proximity of the bound ligand (within 5 Å) playing important role in stabilizing DM via H-bonds and electrostatic interactions. For instance, Ser193 is in suitable position to be involved in making H-bonds with amino group of the sugar moiety. Basic amino acids like Arg144, Arg145 and Lys190 in the vicinity of DM can be targets for interactions with negatively charged carbonyl oxygen functions of the dihydroxyanthraquinone moiety. The hydrogen-bonding or electrostatic interaction acts as an "anchor", intensely determining the 3D space position of DM in the binding pocket and facilitating the hydrophobic interaction of the dihydroxyanthraquinone rings with the side chain of protein. This mode of binding allows hydrogen bonding and electrostatic, hydrophobic interactions to contribute to the binding energy. At this site, the conformation of ligand differs from that in aqueous solution, where the mean plane of the sugar is perpendicular to the dihydroxyanthraquinone plane. Indeed, the finding by CD spectra strongly suggested that glycosidic linkage (C(6a)–C(7)–O(7)–C(1′)) has changed in DM binding biomacromolecule [14]. It is worth mentioning that the docking procedure did not place ligand molecule within site I or II. Moreover, the docked DM molecule is also not posi-

tioned at the third classical-drug binding site (named site III) according to the crystal structure of HSA–hemin determined by recent X-ray study [39]. The modeling study showed that DM binds serum to a non-classical surface binding site. This result is supported by previous studies, which found that warfarin, diazepam and hemin, as marker ligands of sites I, II and III, respectively, show no competition with anthracyclines [7].

4. Conclusions

Interaction between daunomycin with human serum albumin was investigated by the cuvette-based IAsys biosensor and fluorescence spectroscopy. The IAsys biosensor was used to study the interaction of DM with appropriate immobilized HSA in real-time, thus avoiding the artificial changes in binding properties resulting from the instability of anthracycline in some conventional methods. The binding constants of DM with HSA were determined by IAsys biosensor at different temperatures. Furthermore, the binding of DM to HSA is exothermic and favored by both in enthalpy and entropy based on the integrated van't Hoff analysis. DM shows a pH-dependent binding affinity to HSA, as evident from fluorescence quenching studies. The DM binding properties of HSA was also mapped by molecular modeling. Docking calculations found DM to be located at the superficial site within subdomain IB: a non-classical drug binding site. The model showed the microenvironment of DM to be rich in polar (basic) amino acid residues able to stabilize the ligand.

Acknowledgements

We are indebted to Dr. Li Zhang in Central China Normal University for technical assistance in using the SGI workstation and Sybyl software. This work was supported by the National Natural Science Foundation of China (Grant No. 30370366).

References

[1] X.M. He, D.C. Carter, Nature 358 (1992) 209–215.
[2] D.C. Carter, J.X. Ho, Adv. Protein Chem. 45 (1994) 153–203.
[3] G. Sudlow, D.J. Birkett, D.N. Wade, Mol. Pharmacol. 12 (1976) 1052–1061.
[4] J.B. Chaires, in: W., Priebe, (Eds.), Anthracycline Antibiotics: New Analogues, Methods of Delivery and Mechanisms of Action, ACS Symposium Series 574, American Chemical Society, Washington, DC, 1995, pp. 156-167.
[5] L. Trynda-Lemiesz, H. Kozlowski, Bioorg. Med. Chem. 4 (1996) 1709–1713.
[6] O. Chassany, S. Urien, P. Claudepierre, G. Bastian, J.P. Tillement, Cancer Chemother. Pharmacol. 38 (1996) 571–573.
[7] L. Messori, F. Piccioli, S. Gabrielli, P. Orioli, L. Angeloni, C. Di Bugno, Bioorg. Med. Chem. 10 (2002) 3425–3430.
[8] D.S. Hage, J. Austin, J. Chromatogr. A 739 (2000) 39–54.
[9] J. Østergaard, N.H.H. Heegaard, Electrophoresis 24 (2003) 2903–2913.
[10] R.L. Rich, Y.S. Day, T.A. Morton, D.G. Myszka, Anal. Biochem. 296 (2001) 197–207.
[11] C. Bertucci, S. Cimitan, J. Pharm. Biomed. Anal. 32 (2003) 707–714.
[12] C. Bertucci, S. Cimitan, Farmaco 58 (2003) 901–908.
[13] A. Battaglia, C. Bertucci, E. Bombardelli, S. Cimitan, A. Guerrini, P. Morazzoni, A. Riva, Eur. J. Med. Chem. 38 (2003) 383–389.
[14] L. Gallois, M. Fiallo, A. Garnier-Suillerot, Biochim. Biophys. Acta 1370 (1998) 31–40.
[15] J. González-Jiménez, G. Frutos, I. Cayre, M. Cortijo, Biochemie 73 (1991) 551–556.
[16] J.B. Charies, N. Dattagupta, D.M. Crothers, Biochemistry 21 (1982) 3927–3932.
[17] IAsys Technical Resources, Affinity Sensors, Inc. Cambridge, 2001.
[18] D.A. Dmitriev, Y.S. Massino, O.L. Segal, J. Immunol. Methods 280 (2003) 183–202.
[19] G.M. Morris, D.S. Goodsell, R.S. Halliday, R. Huey, W.E. Hart, R.K. Belew, A.J. Olson, J. Comput. Chem. 19 (1998) 1639–1662.
[20] H.M. Berman, J. Westbrook, Z. Feng, G. Gilliland, T.N. Bhat, H. Weissig, I.N. Shindyalov, P.E. Bourne, Nucleic Acids Res. 28 (2000) 235–242.
[21] SYBYL Software, Version 6.9.2, Tripos Associated, Inc. St. Louis, 2003.
[22] T. Peters Jr., Adv. Protein Chem. 37 (1985) 161–245.
[23] A.H. Lin, Y.M. Qin, G.L. Zou, Acta Chim. Sin. 63 (2005) 153–156 (in Chinese).
[24] H. Naghibi, A. Tamura, J.M. Sturtevant, Proc. Natl. Acad. Sci. U.S.A. 92 (1995) 5597–5599.
[25] Y.F. Liu, J.M. Sturtevant, Protein Sci. 4 (1995) 2559–2561.
[26] G. Zeder-Lutz, E. Zuber, J. Witz, M.H.V. Van Regenmortel, Anal. Biochem. 246 (1997) 123–132.
[27] H. Ohtaka, A. Velazquez-Campoy, D. Xie, E. Freire, Protein Sci. 11 (2002) 1908–1916.
[28] P.D. Ross, S. Subramanian, Biochemistry 20 (1981) 3096–3102.
[29] A. Hatsumi, G. Michitaka, Y. Magobei, Thermochim. Acta 251 (1995) 379–388.
[30] J.R. Lakowicz, Principles of Fluorescence Spectroscopy, Plenum Press, New York, 1983, pp. 257–265.
[31] J.R. Lakowicz, G. Weber, Biochemistry 12 (1973) 4161–4170.
[32] W.R. Ware, J. Phys. Chem. 66 (1962) 455–458.
[33] G.Z. Chen, X.Z. Huang, J.G. Xu, Z.B. Wang, Z.X. Zheng, Method of Fluorescent Analysis, second ed., Science Press, Beijing, 1990, pp. 115–120.
[34] H.S. Kim, D.S. Hage, J. Chromatogr. B 816 (2005) 57–66.
[35] D. Yeung, A. Gill, C.H. Maule, R.J. Davies, Trends Anal. Chem. 14 (1995) 49–56.
[36] J. Fisher, K. Ramakrishnan, K.E. McLane, Biochemistry 21 (1982) 6172–6180.
[37] L.M. Hugo, EMBO J. 16 (1997) 1475–1483.
[38] D. Zhong, S.K. Pal, C. Wan, A.H. Zewail, Proc. Natl. Acad. Sci. U.S.A. 98 (2001) 11873–11878.
[39] P.A. Zunszain, J. Ghuman, T. Komatsu, E. Tsuchida, S. Curry, BMC Struct. Biol. 3 (2003) 6–14.